Characteristics of Ammonia Permeation Through Porous Silica Membranes

Masakoto Kanezashi, Akira Yamamoto, Tomohisa Yoshioka, and Toshinori Tsuru
Dept. of Chemical Engineering, Hiroshima University, Higashi-Hiroshima 739-8527, Japan

DOI 10.1002/aic.12059
Published online October 22, 2009 in Wiley InterScience (www.interscience.wiley.com).

A sol–gel method was applied for the preparation of silica membranes with different average pore sizes. Ammonia (NH_3) permeation/separation characteristics of the silica membranes were examined in a wide temperature range (50–400°C) by measurement of both single and binary component separation. The order of gas permeance through the silica membranes, which was independent of membrane average pore size, was as follows: $He > H_2 > NH_3 > N_2$. These results suggest that, for permeation through silica membranes, the molecular size of NH_3 is larger than that of H_2, despite previous reports that the kinetic diameter of NH_3 is smaller than that of H_2. At high temperatures, there was no effect of NH_3 adsorption on H_2 permeation characteristics, and silica membranes were highly stable in NH_3 at 400°C (i.e., gas permeance remained unchanged). On the other hand, at 50°C NH_3 molecules adsorbed on the silica improved NH_3-permselectivity by blocking permeation of H_2 molecules without decreasing NH_3 permeance. The maximal NH_3/H_2 permeance ratio obtained during binary component separation was ~30 with an NH_3 permeance of $\sim 10^{-7}$ mol m^{-2} s^{-1} Pa^{-1} at an H_2 permeation activation energy of ~6 kJ mol^{-1}. *AIChE J,* 56: 1204–1212, 2010
Keywords: silica membrane, sol–gel method, ammonia permeation, adsorption, stability

Introduction

Recovery of ammonia (NH_3) produced by the Haber process, from mixtures of N_2, H_2, and other inert gases, is a critical unit operation in NH_3 synthesis plants. During the synthesis of NH_3, the reaction of N_2 and H_2 is conducted at 450°C and 14 MPa using an iron-based catalyst. The production streams in the reactor, which are ~16% NH_3, are cooled to 60°C. In conventional NH_3 synthesis, these streams are subsequently cooled to 38°C to condense additional NH_3. This process requires a large amount of energy to both cool the product and reheat the unreacted H_2 and N_2, which are recycled, to 450°C. Membrane-based separation is an attractive alternative, as it is a simple and energy-conserving method. Membrane separation has many advantages, especially for gas separation with no phase change. If NH_3 can be selectively separated from the production stream at high temperatures using NH_3-permselective membranes, then simple methods for the synthesis of NH_3 that use much less energy are feasible. The key to realization of such novel methods is the development of NH_3-permselective membranes that have high thermal and chemical stability and excellent NH_3 separation performance (permeance and selectively).

Only a few studies have examined the NH_3 permeation properties of organic or inorganic membranes because measurement of NH_3 permeance is difficult.[1–4] Tricoli and Cussler[2] reported that organic membranes, such as perfluorosulfonic acid and polyvinylammonium thiocyanate, are highly NH_3/H_2-selective at 25–60°C. However, utilization of organic polymer membranes during high-temperature synthesis of NH_3 is limited by the poor thermal stability of organic polymer networks. Compared with organic polymer membranes, inorganic membranes have potential for application in high-temperature, gas separation processes because of their high thermal stability. There are two types of NH_3-permselective inorganic membranes: molten salt membranes[3]

Correspondence concerning this article should be addressed to M. Kanezashi at kanezashi@hiroshima-u.ac.jp or T. Tsuru at tsuru@hiroshima-u.ac.jp.

and porous inorganic membranes, such as silica or zeolite.[4] In 1992, Burban and coworkers[3] first reported the NH_3 permeation behavior of molten $LiNO_3$ and $ZnCl_2$ membranes. Molten $LiNO_3$ and $ZnCl_2$ membranes showed an NH_3 permeance of $\sim 10^{-9}$–10^{-8} mol m^{-2} s^{-1} Pa^{-1} with a high NH_3/N_2 selectivity of 80–1000 at 250–300°C. However, NH_3 separation performance (permeance, NH_3/N_2 selectivity) was highly dependent on the partial pressure of the NH_3 feed, that is, both NH_3 permeance and NH_3/N_2 selectivity decreased drastically as NH_3 feed partial pressure increased. A plausible explanation for this observation is chemically facilitated transport with lithium ammoniate complexes, $Li(NH_3)^+$, as the carrier species.

To examine both NH_3 separation performance and NH_3 permeation behavior of porous inorganic membranes, Camus et al.[4] fabricated MFI-type zeolite and methylated silica membranes. At 80°C, MFI-type zeolite membranes showed a high NH_3 permeance of 2.1×10^{-7} mol m^{-2} s^{-1} Pa^{-1} with a NH_3/H_2 selectivity of about 10, whereas the NH_3 permeance of the silica membranes was much greater, 7.6×10^{-7} mol m^{-2} s^{-1} Pa^{-1}, with a NH_3/H_2 selectivity of $\sim$7. The NH_3/H_2 selectivity for both silica and MFI-type zeolite membranes increased with temperature as high as 80°C. However, no published studies have examined the NH_3 permeation behavior of porous inorganic membranes in a wide temperature range, especially at high temperatures. A more thorough investigation is required to understand the characteristics of NH_3 permeation through porous inorganic membranes in greater detail. At high temperatures (under negligible adsorption atmosphere), NH_3 molecules should be separated from gaseous mixtures of NH_3, H_2, and N_2 by a molecular sieving mechanism, which might be highly dependent on the relationship between the molecular size of the permeating gases (NH_3, H_2, and N_2) and membrane pore size. Reportedly, the order of the kinetic diameters for NH_3, H_2, and N_2, which were obtained using the Stockmayer potential, is as follows: NH_3 (0.26 nm), H_2 (0.289 nm), and N_2 (0.364 nm).[5] On the other hand, Leeuwen,[6] also using the Stockmayer potential, determined the molecular size of NH_3 to be 0.326 nm. If the molecular size of NH_3 is 0.26 nm[5] during permeation through porous inorganic membranes, then NH_3 molecules could be selectively separated from gaseous mixtures of NH_3 and H_2 by molecular sieving. By contrast, if the molecular size of NH_3 is 0.326 nm,[6] then the mechanism of selective NH_3 separation would be preferential adsorption of NH_3 and blocking of H_2 molecules. In either case, the MFI-type zeolite structure, which contains both a straight channel (0.54 nm $\times$ 0.56 nm) and a sinusoidal channel (0.51 nm $\times$ 0.55 nm),[7] appears too large for separation of NH_3 molecules from gaseous mixtures of NH_3 and H_2. Under a negligible adsorption atmosphere (at high temperatures), permeation behaviors should follow a Knudsen-type mechanism because of a small ratio of kinetic diameter of the diffusing gas (NH_3: 0.26 nm, H_2: 0.289 nm) to the zeolite channel size, λ ($=d_m/d_p$).[8–10]

The NH_3 separation performance of amorphous silica membranes is expected to be superior to that of MFI-type zeolite membranes because the pore size of silica membranes relative to the size of the separation components can easily be controlled. Sol–gel and chemical vapor deposition methods have been applied to the preparation of silica membranes on porous substrates.[11–22] In general, sol–gel methods have greater flexibility in the control of the size of the pores in the silica membranes. Several research groups have reported the preparation of various separation membranes with controlled pore size in the range of 0.3–0.5 nm, for example, H_2/N_2, CO_2/CH_4, C_3 isomers, H_2/C_3H_8 separation, etc.[15,17–19,21,22] This article reports both the fabrication of sol–gel-derived silica membranes with different average pore sizes and the evaluation of gas permeation/separation behavior (He, NH_3, H_2, N_2, and SF_6) in a wide temperature range (50–400°C). Membrane stability in NH_3 at high temperatures was also evaluated by determination of the time course of gas permeance.

Experimental

Fabrication of silica membranes using a sol–gel method

Silica colloidal sols were prepared as previously described.[23] Tetraethoxysilane (TEOS) was added to water with nitric acid as a catalyst at molar ratios of $TEOS/H_2O/HNO_3$ = 0.1:11.5–23:0.016–0.033, and then the solutions were hydrolyzed at room temperature for 12 h. To convert the polymeric sols to colloidal sols, additional nitric acid and water were added, and the solutions were boiled for an additional 8 h, keeping the total amount of solution constant. The final sols contained 2.0, 1.5, and 1.0 wt % of TEOS with colloidal diameters of 45, 30, and 18 nm, respectively, as determined by laser diffraction methods (ELS800, Otsuka Electric, Japan). It was found that the particle sizes of silica colloidal sols could be controlled by the concentration of the starting TEOS in the sol solution.[23] Powdered samples of the silica gels were prepared by dripping the colloidal sols onto a platinum plate heated to 180°C, followed by calcination at 550°C in air for 30 min. Temperature programmed desorption (TPD) was conducted to evaluate the desorption of NH_3 from the silica gel powder. After pretreatment at 500°C for 1 h under flow of He and subsequent cooling to room temperature, the silica gel powder was exposed to NH_3 flow (10 cc min^{-1}) at room temperature for 1 h. TPD was conducted at a ramping rate of 15°C min^{-1}, and the concentrations of outlet gases released from the reactor were measured by mass spectrometry in He using Ar gas as a standard.

Silica membranes were fabricated by coating porous substrates with silica colloidal sols. Porous α-alumina tubes (porosity: 50%, average pore size: 1 μm) were used as the silica membrane supports. After the formation of a silica-zirconia (SiO_2-ZrO_2) intermediate layer, which reportedly has an average pore size of $\sim$1–2 nm,[24–26] three kinds of silica colloidal sols diluted to less than 0.5 wt % were coated the SiO_2-ZrO_2 intermediate layer and calcined at 550°C in air for 30 min. The coating and calcination procedures were repeated several times for each colloidal sol, from a sol with large particle size to a smaller one to form a crack-free, active silica layer for gas separation.

Measurement of gas permeation/separation of the silica membranes

Figure 1 shows a schematic diagram of the experimental apparatus used for the measurement of gas permeation/separation. A single industrial-grade gas (He, H_2, CO_2, N_2, and

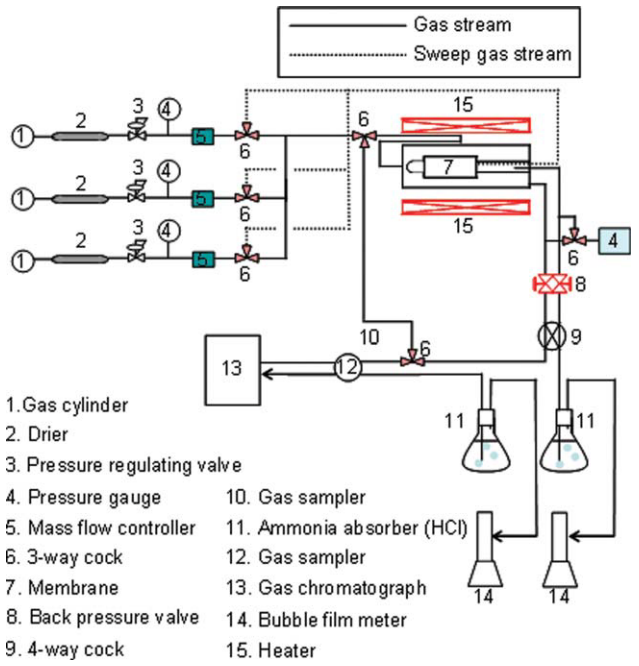

Figure 1. Schematic diagram of the experimental apparatus used for gas permeation/separation.

[Color figure can be viewed in the online issue, which is available at www.interscience.wiley.com.]

SF_6) was fed into the apparatus outside (upstream) of a cylindrical membrane module at 200–300 kPa, while the downstream pressure was held constant at atmospheric pressure. The temperature of the membrane cell was controlled using an electric furnace and kept constant at a specified temperature between 50 and 400°C. The permeation rate was measured using a bubble film meter (Method 1). In the case of NH_3 permeation, a sweep gas (Ar) was used (Method 2). NH_3 was fed upstream at atmospheric pressure, whereas the sweep gas (Ar, flow rate: 100 cc min^{-1}) was fed downstream at atmospheric pressure. The composition of the retentate and permeate gases was analyzed by gas chromatography with a TCD detector (column: Porapak N (GL Science, Japan)). Gas flow rates were measured using bubble film meters after removal of NH_3 with HCl.

Results and Discussion

Gas permeation characteristics of porous silica membranes

Figure 2 shows an SEM image of a silica membrane cross-section. A thin, continuous silica separation layer can be seen on top of the SiO_2-ZrO_2 intermediate layer, while the thickness of the active separation layer is clearly less than 1 μm.

The pore size distribution of the porous silica membranes was estimated by measuring the permeance of several gases at 200°C, at which temperature the effect of surface flow is negligible. Figure 3 shows the gas permeance for the silica membranes (Si-1, Si-2, and Si-3) at 200°C as a function of kinetic diameter. It should be noted that there is no difference in gas permeance that was measured by Method 1 (closed symbols) compared with that measured using Method 2 (open symbols). The Si-1 membrane showed a high hydrogen permeance of 2.16 × 10^{-6} mol m^{-2} s^{-1} Pa^{-1} with a high H_2/SF_6 permeance ratio of 1600 and low H_2/N_2 permeance ratio (~30) at 200°C. On the other hand, the H_2 permeance of the Si-3 membrane was one order of magnitude less than that of the Si-1 membrane with a high H_2/N_2 permeance ratio of 1000. It should be noted that the permeance of SF_6 through the Si-3 membrane was less than 10^{-10} mol m^{-2} s^{-1} Pa^{-1}, which is the detection limit of this gas permeation system. For the Si-2 membrane, He permeance was comparable to that of the Si-1 membrane. The Si-2 membrane had a H_2/N_2 permeance ratio of ~100 and a H_2/SF_6 permeance ratio of 2500; thus, the selectivity of the Si-2 membrane was higher than that of the Si-1 membrane, but lower than that of the Si-3 membrane. The average pore size of the Si-1 membrane was estimated to be ~0.5–0.6 nm, whereas that of the Si-3 membrane was ~0.3 nm and that of the Si-2 membrane 0.4–0.5 nm. These results suggest that a high H_2/N_2 permeance ratio can be obtained by use of membranes with an average pore size of 0.3 nm, whereas high

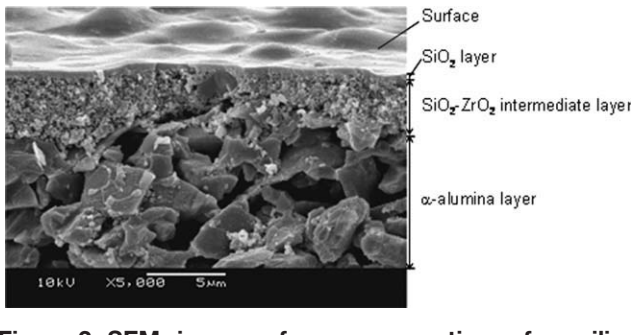

Figure 2. SEM image of a cross-section of a silica membrane.

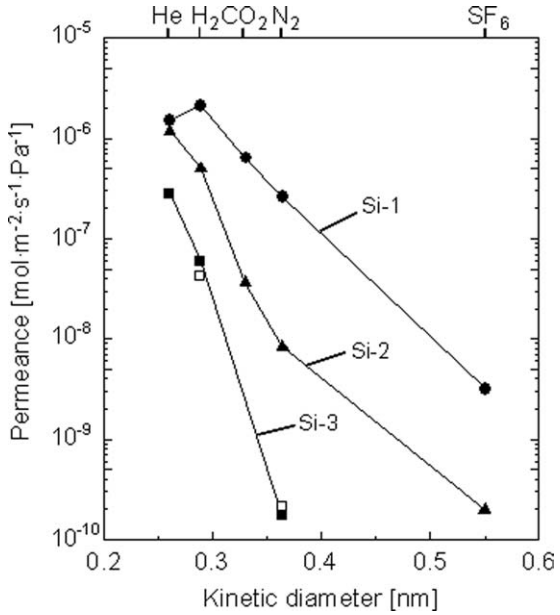

Figure 3. Gas permeances for the silica membrane (Si-1, Si-2, and Si-3) at 200°C as a function of kinetic diameter.

(Closed symbols: gas permeances obtained by Method 1; open symbols: gas permeances determined using Method 2).

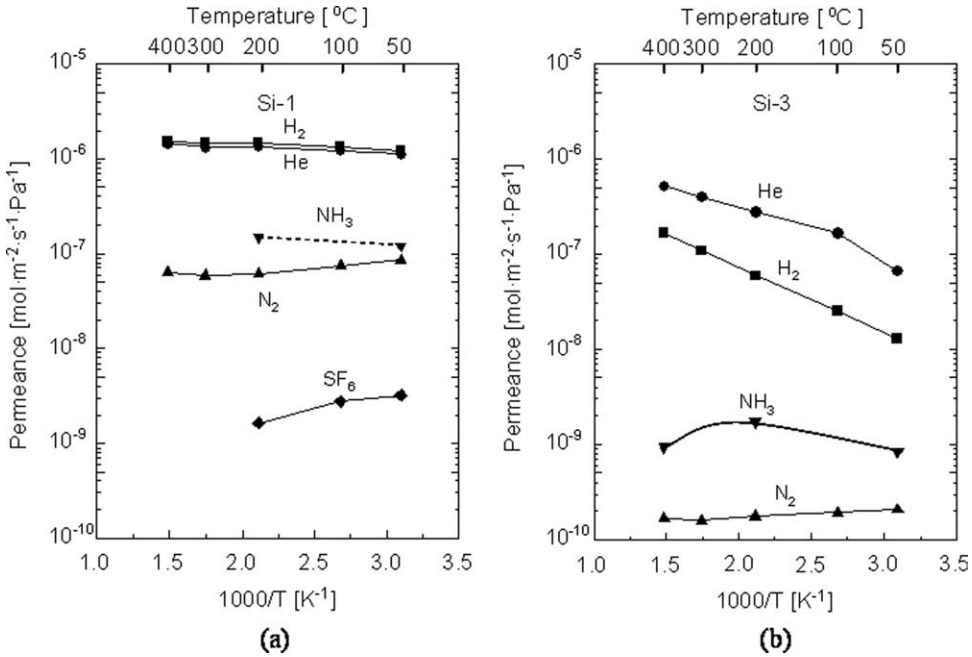

Figure 4. Temperature dependence of gas permeances for the Si-1 membrane (a) and the Si-3 membrane (b) in the temperature range of 50–400°C.

H_2/SF_6 permeance ratios can be achieved using membranes with a much larger average pore size. The average pore size of the silica membranes was successfully controlled by using colloidal sols with different colloidal diameters.

Figure 4 shows the temperature dependence of gas permeance for both the Si-1 membrane (a) and the Si-3 membrane (b) at temperatures ranging between 50 and 400°C. For the Si-1 membrane, He and H_2 permeances were independent of temperature, whereas those for the Si-3 membrane increased markedly with temperature, because of the activated permeation mechanism. For the Si-3 membrane, NH_3 permeation was maximal at 200°C. N_2 permeance through the Si-1 and Si-3 membranes showed Knudsen-type permeation behavior: permeance increased slightly with decreasing temperature. The permeance of SF_6 through the Si-1 membrane also exhibited Knudsen-type permeation behavior.

The difference in He and H_2 permeation behavior between the Si-1 and Si-3 membranes can be attributed to the differences in average pore size and pore size distribution. It is known that sol–gel-derived silica membranes are composed of both pores in the silica particles, which form by amorphous silica networks, and interparticle pores, which are formed by spaces between gel particles.[18] Small molecules, such as He and H_2, permeate both the silica networks and the interparticle pores, whereas slightly larger molecules, such as N_2 and SF_6, can only permeate through the interparticle pores. Because the size of the pores in the silica networks is similar to the molecular size of He and H_2, these molecules permeate through the silica networks by the activated permeation mechanism. For translocation through interparticle pores, He and H_2 molecules permeate by the Knudsen mechanism because the interparticle pores are much larger than the He and H_2 molecules. Permeation behavior is thought to be governed by the balance between activated and Knudsen permeation. Therefore, the flow rate through interparticle pores of the Si-3 membrane by Knudsen permeation is much less than that of the Si-1 membrane because the average pore size of the Si-3 membrane is less than that of the Si-1 membrane. The maximum point of NH_3 permeance can be explained as follows: the number of adsorbed molecules decreases with increasing temperature (above the maximum), whereas at low temperatures, especially below the critical temperature of NH_3 (<130°C), the mobility of adsorbed molecules decreases because of the liquid-like diffusion of the pore-filling molecules.[27] The TPD curve of silica gel powder after exposure to an NH_3 atmosphere is shown in Figure 5. The amount of desorbed NH_3

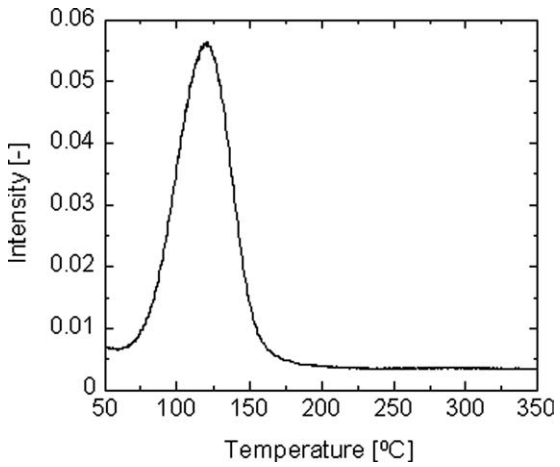

Figure 5. Temperature programmed desorption (TPD) curve of a silica gel powder after exposure to an NH_3 atmosphere (ramping rate: 15°C min^{-1}).

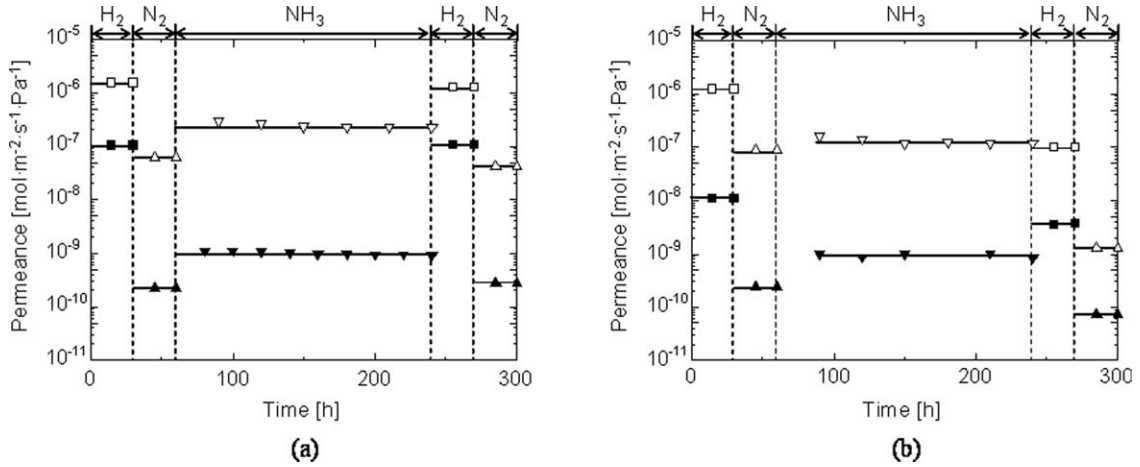

Figure 6. Time course of gas permeance (H_2, N_2, and NH_3) at 400°C (a) and 50°C (b).

(Open symbols: gas permeances for the Si-1 membrane; closed symbols: gas permeances for the Si-3 membrane).

increased drastically at temperatures less than 130°C, which is the critical temperature, and decreased at temperatures greater than 130°C. The TPD results are highly consistent with the characteristics of NH_3 permeation through silica membranes.

Reportedly, the order of kinetic diameter for He, H_2, NH_3, and N_2 is as follows: He (0.26 nm), NH_3 (0.26 nm), H_2 (0.289 nm), and N_2 (0.364 nm).[5] By contrast, the order of gas permeance for the silica membranes, which was independent of average pore size, was He > H_2 > NH_3 > N_2. Both silica membranes showed permselectivity for H_2 over NH_3: the H_2/NH_3 permeance ratio for the Si-1 membrane at 200°C was 6, whereas the ratio for the Si-3 membrane at 200°C was 40 and at 400°C was 178, due to activated permeation of H_2 molecules. For spherical and nonpolar molecules, such as He, H_2, and N_2, the Lennard-Jones potential was used to obtain the kinetic diameter, which is defined as the shortest possible intermolecular distance between two approaching molecules.[5] For polar molecules, such as H_2O and NH_3, the Stockmayer potential, which considers both electric dipole interactions and the Lennard-Jones potential, is widely used for calculation of molecular size. The parameters for both potentials were determined from second virial coefficients or gas viscosity data by considering adsorption by zeolite.[5] When NH_3 molecules permeate an amorphous silica structure with a pore diameter of 0.3–0.5 nm at high temperatures, the interaction between NH_3 molecules and amorphous silica is dominant, that is, the interaction between NH_3–NH_3 molecules (mean free path: 220 nm, 500°C, 101.3 kPa) is weaker than that between NH_3 molecules and amorphous silica. Therefore, the concentration of NH_3 molecules in a membrane is thought to be quite low due to both the mean free path of the NH_3 molecules (220 nm: 500°C, 101.3 kPa) and the positive activation energy of NH_3 permeation. This suggests that the electric dipole interaction between NH_3 molecules can be neglected because of the low concentration of NH_3. Thus, it is possible that the actual molecular size of NH_3 is much larger than 0.26 nm because of the reduced electric dipole interaction. Leeuwen[6] determined the molecular size of NH_3 to be 0.326 nm using a Gibbs ensemble Monte Carlo simulation technique, taking into account the derivation of the Stockmayer potential parameters. Stockmayer parameters were derived by relating the critical temperature and one liquid density point of the real fluid to those of a corresponding Stockmayer fluid, resulting in a reduced dipole moment. A molecular size of 0.326 nm seems reasonable for NH_3 during permeation of silica. This finding explains the difficulty associated with selective separation of NH_3 molecules from H_2–NH_3 gas mixtures using a molecular sieving mechanism.

Effect of NH_3 permeation on membrane performance

Figure 6 shows the time course of gas permeance through the Si-1 and Si-3 membranes at 400°C (a) and 50°C (b). Before NH_3 permeation through the silica membranes, N_2 and H_2 were fed to silica membranes for 30 min, confirming the constant permeances of N_2 and H_2 and the thermal stability of the amorphous silica structure at 400°C. Then, NH_3 was fed to silica membranes for about 3 h, followed by N_2 and H_2 measurement, to examine the effect of NH_3 on membrane performance. For both membranes, NH_3 permeance was constant for up to 180 min. At 400°C, the permeances of N_2 and H_2 after NH_3 permeation were similar to values measured before NH_3 permeation. This result suggests that, at 400°C, exposure to an NH_3 atmosphere does not alter the membrane structure, that is, the silica membrane is highly stable in NH_3 at 400°C. The same experiment was conducted at 50°C (Figure 6b). After NH_3 permeation at 50°C for 180 min, the permeances of H_2 and N_2 were ~90 and 40% of their initial values for the Si-1 and Si-3 membranes, respectively. The Si-1 membrane, which had a larger average pore size, showed a greater decrease in permeance than the Si-3 membrane, probably because of greater NH_3 adsorption by the silica (amorphous silica networks and interparticle pores). These results suggest that NH_3 adsorption by silica can significantly affect the separation of NH_3 from H_2 gaseous mixtures.

Figure 7 shows the temperature dependence of gas permeances for the Si-2 membrane at temperatures ranging between 50 and 400°C. Before binary component gas separation (H_2–NH_3, N_2–NH_3 gas mixture), the permeances of H_2

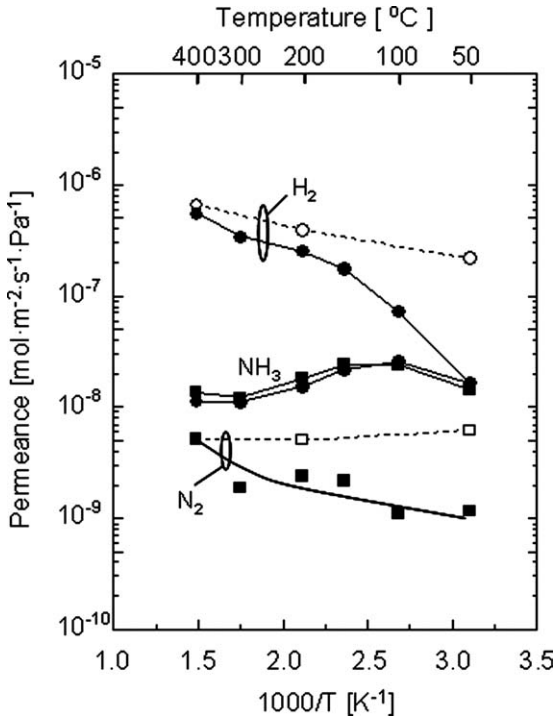

Figure 7. Temperature dependence of gas permeances for the Si-1 membrane in the temperature range of 50–400°C.

(Open symbols on broken line: gas permeances obtained by single gas permeation; closed symbols on solid line: gas separation obtained by binary component separation). The conditions of the binary separation experiments were as follows: feed gas composition, $NH_3/H_2 = 1{:}1$ (circle symbols), $NH_3/N_2 = 1{:}1$ (square symbols); P_{feed}, 100 kPa, $P_{permeate}$, 100 kPa; and sweep flow rate, 100 cc min^{-1}.

and N_2 were measured using single gas permeation (open symbols on broken line). For single gas permeation, the permeance of H_2 increased with increasing temperature, whereas that of N_2 increased slightly with decreasing temperature (the same trend as in Si-3 membrane). There was no difference in NH_3 permeance measured by separation of H_2–NH_3 mixtures (closed circle symbols) or of N_2–NH_3 mixtures (closed square symbols), because NH_3 permeance was independent of the presence of other molecules. For the Si-2 membrane, NH_3 permeance was maximal between 100 and 150°C. The Si-3 membrane showed a similar trend with a maximum at ~200°C (in Figure 4b). The difference in NH_3 permeance maxima can be explained as follows. Because of the difference in average pore size (Si-2 > Si-3), it is expected that NH_3 molecules can easily plug pores in the Si-3 membrane at higher temperatures.

A large difference between H_2 and N_2 permeation was observed; this difference was especially pronounced at temperatures below 200°C. At less than 200°C, H_2 permeance obtained by separation of H_2–NH_3 mixtures was markedly less than that obtained by single gas permeation. This is probably because blocking by NH_3 adsorption is enhanced at lower temperatures. The permeance of N_2 obtained by separation of N_2–NH_3 mixtures was also less than that determined by single permeation because of the increased blocking effect at lower temperatures. This result suggests that adsorbed NH_3 molecules in a membrane improve NH_3-permselectivity by blocking the permeation of other molecules, such as H_2 molecules, without decreasing NH_3 permeance.

NH_3 separation performance measured by binary component gas separation

Binary separation of NH_3 and H_2 gases was conducted using the Si-1 membrane. Figure 8 shows the gas permeance of H_2 and NH_3 through the Si-1 membrane as a function of the mole fraction of NH_3 in the feed at 400°C (a) and 50°C (b). At 400°C, H_2 and NH_3 permeances were constant and independent of the mole fraction of NH_3 in the feed. At high temperatures, adsorption of NH_3 by silica was negligible, such that H_2 molecules freely permeated the silica membranes. For binary component separation of NH_3 and H_2 at 50°C, however, the permeance of H_2 decreased drastically even when the mole fraction of NH_3 in the feed was less than 0.4, whereas NH_3 permeance remained constant when the mole fraction was greater than 0.4. As shown in Figure 4, the Si-1 membrane shows H_2-permselectivity during single gas permeation (H_2/NH_3 permeance ratio: ~10) because the molecular size of H_2 is less than that of NH_3. On the

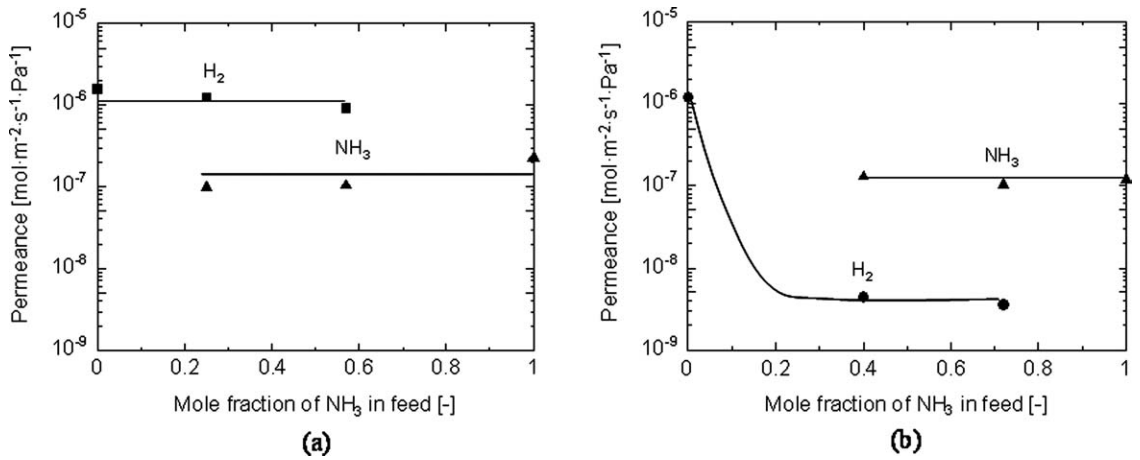

Figure 8. H_2 and NH_3 permeances for the Si-1 membrane as a function of the mole fraction of NH_3 in the feed at 400°C (a) and 50°C (b).

Table l. Single and Binary Component Separation for the Si-1, Si-2, and Si-3 Membranes at 50 and 400°C

		Single Gas permeation			Binary component separation*		
	Temperature [°C]	H_2 Permeance [10^{-8} mol m^{-2} s^{-1} Pa^{-1}]	NH_3 Permeance [10^{-8} mol m^{-2} s^{-1} Pa^{-1}]	H_2/NH_3 Permeace Ratio	H_2 Permeance [10^{-8} mol m^{-2} s^{-1} Pa^{-1}]	NH_3 Permeance [10^{-8} mol m^{-2} s^{-1} Pa^{-1}]	NH_3/H_2 Permeace Ratio
Si-1	50	134	124	10.8	0.355	10.2	28.7
	400	143	–	–	126	10.4	0.083
Si-2	50	22.1	1.12	19.7	1.65	1.68	1.02
	400	66.5	1.31	50.8	63.5	1.17	0.018
Si-3	50	1.31	0.0843	15.4	0.168	0.0521	0.31
	400	16.7	0.0938	178	–	–	–

*Feed gas composition: NH_3H_2 = 1:1.

other hand, during binary component separation, the Si-1 membrane showed NH_3-permselectivity because of NH_3 blocking of H_2 permeation (NH_3/H_2 permeance ratio: 30). Table 1 summarizes the results of the single and binary component separation for the Si-1, Si-2, and Si-3 membranes at 50 and 400°C. It should be noted that, based on the results of the single gas permeation experiment, the Si-3 membrane was expected to show a H_2-permselectivity of 178 relative to NH_3 during binary separation.

The effect of NH_3 adsorption to silica on H_2 permeation of a membrane is highly dependent on the pore size of the silica membranes. In this study, NH_3 separation performance was examined by conducting binary component separation using several silica membranes that differed in average pore size. The activation energy of H_2 permeation (E_p) was obtained by regressing Eq. 1[28] with the experimental single permeation data at temperatures above 200°C.

$$P = \frac{k_0}{\sqrt{MRT}} \exp\left(-\frac{\Delta E_p}{RT}\right) \tag{1}$$

where k_0 is a characteristic constant of the porous membrane, such as membrane thickness, porosity, or tortuosity, M is the molecular weight of the permeating gas, R is the gas constant, and T is the temperature. When H_2 molecules permeate through amorphous silica structure by activated permeation, they have to overcome the energy barrier imposed by the amorphous silica structure. Because the activation energy of H_2 permeation (E_p) is determined by pore size and by the interactions between H_2 molecules and the pore wall in a membrane, E_p is suitable for determination of the pore size that permits permeation of H_2 molecules, that is, activation energy increases as pore size decreases because of the larger repulsive force.[8–10,23–26,29,30] At the same time, pore size distribution of silica membranes strongly affects the magnitude of activation energy because of the balance between Knudsen and activated permeation mechanisms.

Figure 9 shows the NH_3/H_2 permeance ratio obtained by binary component separation (feed gas composition: NH_3/H_2 = 1:1) at 50°C as a function of the activation energy of H_2 permeation. The upper part of this figure shows H_2 and NH_3 permeances obtained by binary component separation. The permeances of H_2 and NH_3 decreased with increasing activation energy of H_2 permeation because of the decrease in the pore size of the silica membranes. The NH_3/H_2 permeance ratio reached a maximum at an H_2 permeation activation energy of ~6 kJ mol^{-1}. In the case of membranes with activation energy greater than 10 kJ mol^{-1}, the NH_3/H_2 permeance ratio decreased with increasing activation energy. This result occurs because at a higher activation energy, which corresponds to a smaller average pore size, NH_3 molecules can no longer permeate through the pores, whereas the smaller H_2 molecules can permeate the membrane. As a result, the blocking effect of NH_3 adsorption on H_2 permeation is reduced. If there are no pinholes in a membrane, the NH_3/H_2 permeance ratio will approach zero (no flow of NH_3). On the other hand, when average pore size is large ($4 < E_p < 10$ kJ mol^{-1}), adsorbed NH_3 molecules

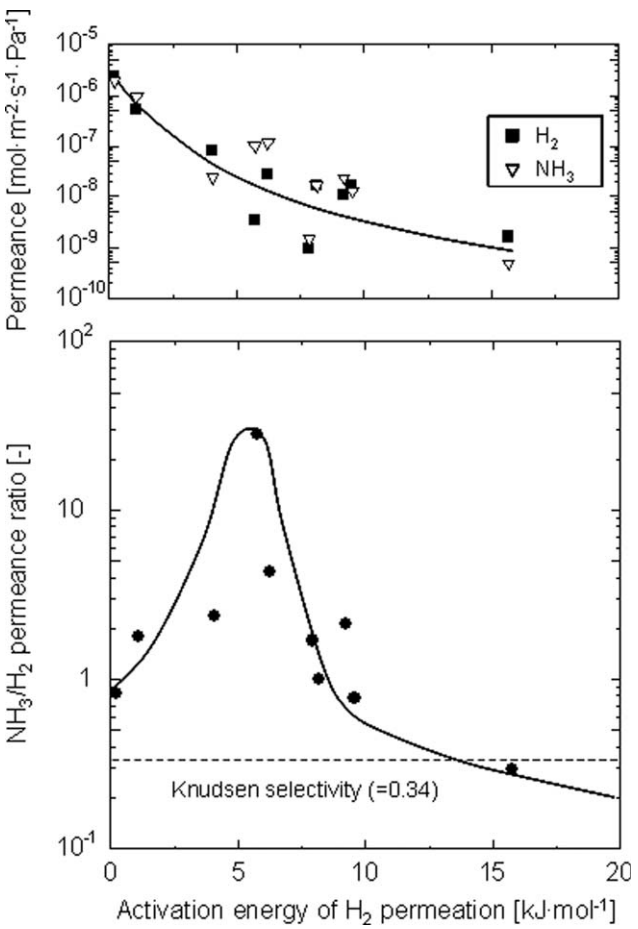

Figure 9. NH_3/H_2 permeance ratio obtained by binary component separation (feed gas composition: NH_3/H_2 = 1:1) at 50°C as a function of the activation energy of H_2 permeation.

effectively prevent permeation of H_2 molecules, thereby increasing the NH_3/H_2 permeance ratio. In the case of membranes with a much larger average pore size (activation energy < 4 kJ mol^{-1}), adsorption of NH_3 molecules no longer blocks permeation of H_2 molecules, and NH_3/H_2 selectivity is reduced. Oyama and coworkers[30] calculated activation energy for permeation of H_2 and He molecules through silica membranes using an ab initio calculation. $H_{2n}Si_nO_n$ ($n = 4$–8) planar silica n-membered rings, corresponding to the pore size of amorphous silica networks, were used to calculate activation energy. There was a good correlation between activation energy and the distance from the center of the ring to the oxygen atoms (pore size of silica n-membered rings), that is, activation energy increased as the number of silica-membered rings decreased.[30] The pore size of amorphous silica networks with an activation energy of H_2 permeation of $\sim$6 kJ mol^{-1}, which had a maximal NH_3/H_2 permeance ratio of 30, was obtained from the correlation curve.[30] The effective pore diameter of amorphous silica networks was calculated using Eq. (2)

$$d_{\text{effective}} = 2r_p - \sigma_o \tag{2}$$

where r_p is the distance from the center of the ring to the oxygen atoms and σ_o is the diameter of an oxygen atom (0.27 nm).[31] The effective pore diameter was $\sim$0.35 nm, which is close to the molecular size of NH_3 (0.326 nm)[6] during permeation through an amorphous silica structure.

Conclusions

A sol–gel method was applied to the preparation of silica membranes with different average pore sizes. The average pore size of the silica membranes was successfully controlled by using colloidal sols with different colloidal diameters. NH_3 permeation/separation characteristics of the silica membranes were examined in a wide temperature range (50–400°C) by measurement of both single and binary component separation. Membrane stability in NH_3 at high temperatures was also evaluated by determination of the time course of gas permeance.

(1) The order of gas permeance for silica membranes was He $>$ H_2 $>$ NH_3 $>$ N_2, which was not consistent with the order of kinetic diameter (He: 0.26 nm, NH_3: 0.26 nm, H_2: 0.289 nm, N_2: 0.364 nm), but was independent of average pore size. This result suggests that the molecular size of NH_3 is larger than that of H_2 in the case of permeation through an amorphous silica structure.

(2) For binary component separation, silica membranes showed H_2 permselective behavior under a negligible NH_3 adsorption atmosphere, for example, H_2/NH_3 permeance ratio: 150 at 400°C. On the other hand, at low temperature silica membranes showed NH_3-permselectivity because NH_3 molecules adsorbed by silica efficiently blocked permeation of H_2 molecules, resulting in an NH_3/H_2 permeance ratio of 30 at 50°C. Moreover, silica membranes were quite stable under an NH_3 atmosphere at 400°C.

(3) The effect of NH_3 adsorption by silica on H_2 permeation was highly dependent on the size of the pores in the silica membranes. In the case of membranes with activation energy greater than 10 kJ mol^{-1}, the NH_3/H_2 permeance ratio decreased with increasing activation energy. By contrast, when the average pore size was increased ($4 < E_p < 10$ kJ mol^{-1}), adsorbed NH_3 molecules effectively prevented permeation of H_2 molecules, resulting in an increase in the NH_3/H_2 permeance ratio ($\sim$30). In the case of membranes with a much larger average pore size (activation energy < 4 kJ mol^{-1}), adsorption of NH_3 molecules no longer blocked permeation of H_2 molecules, and NH_3/H_2 selectivity was reduced.

Based on the above conclusions, NH_3 molecules can be selectivity separated from gaseous mixtures of NH_3 and H_2 by use of amorphous silica membranes with a pore size of $\sim$0.35 nm. Further improvements in NH_3 separation using amorphous silica membranes are as follows: precise control of average pore size and pore size distribution, as well as the enhanced interactions between NH_3 molecules and silica surfaces modified with functional groups and/or metal doping.

Notation

$d_{\text{effective}}$ = effective pore diameter of amorphous silica networks, m
d_m = kinetic diameter of molecules, m
E_p = activation energy for permeation, J mol^{-1}
k_0 = geometrical coefficient, defined by Eq. 1
M = molecular weight, g mol^{-1}
P = permeance, mol m^{-2} s^{-1} Pa^{-1}
P_{feed} = feed (upstream) side pressure, Pa
P_{permeate} = permeate (downstream) side pressure, Pa
r_p = distance from the center of the ring to the oxygen atoms, m
R = gas constant, J mol^{-1} K^{-1}
T = absolute temperature, K

Greek letters

λ = the ratio of kinetic diameter of the diffusion molecule to the zeolite pore diameter, dimensionless
σ_o = diameter of an oxygen atom, m.

Literature Cited

1. He Y, Cussler EL. Ammonia permeabilities of perfluorosulfonic membranes in various ionic forms. *J Membr Sci*. 1992;68:43–52.
2. Tricoli V, Cussler EL. Ammonia selective hollow fibers. *J Membr Sci*. 1995;104:19–26.
3. Laciak DV, Pez GP, Burban PM. Molten salt facilitated membranes. II. Separation of ammonia from nitrogen and hydrogen at high temperatures. *J Membr Sci*. 1992;65:31–38.
4. Camus O, Perera S, Crittenden B, van Delft YC, Meyer F, Pex PPAC, Kumakiri I, Miachon S, Dalmon JA, Tennison S, Chanaud P, Groensmit E, Nobel W. Ceramic membranes for ammonia recovery. *AIChE J*. 2006;52:2055–2065.
5. Breck DW. *Zeolite Molecular Sieves: Structure, Chemistry and Use*. New York: Wiley, 1974:593–724.
6. van Leeuwen ME. Derivation of Stockmayer potential parameters for polar fluids. *Fluid Phase Equilib*. 1994;99:1–18.
7. Flanigen EM, Bennett JM, Grose RW, Cohen JP, Patton RL, Kirchner RM, Smith JV. Silicalite, a new hydrophobic crystalline silica molecular sieve. *Nature*. 1978;271:512–516.
8. Xiao J, Wei J. Diffusion mechanism of hydrocarbons in zeolites. I. Theory. *Chem Eng Sci*. 1992;47:1123–1141.
9. Kanezashi M, O'Brien-Abraham J, Lin YS, Suzuki K. Gas permeation through DDR-type zeolite membranes at high temperatures. *AIChE J*. 2008;54:1478–1486.
10. Kanezashi M, Lin YS. Gas permeation and diffusion characteristics of MFI-type zeolite membranes at high temperatures. *J Phys Chem C*. 2009;113:3767–3774.

11. Gavalas GR, Megris CE, Nam SW. Deposition of H_2-permselective SiO_2 films. *Chem Eng Sci*. 1989;44:1829–1835.
12. Cao G, Lu Y, Delattre L, Brinker CJ, Lopez GP. Amorphous silica molecular sieving membranes by sol-gel processing. *Adv Mater*. 1996;8:588–591.
13. de Vos RM, Maier WF, Verweij H. Hydrophobic silica membranes for gas separation. *J Membr Sci*. 1999;158:277–288.
14. Kusakabe K, Sakamoto S, Saie T, Morooka S. Pore structure of silica membranes formed by a sol-gel technique using tetraethoxysilane and alkyltriethoxysilanes. *Sep Purif Technol*. 1999;16:139–146.
15. Lin YS, Kumakiri I, Nair BN, Alsyouri H. Microporous inorganic membranes. *Sep Purif Method*. 2002;31:229–379.
16. Duke MC, da Costa JCD, Do DD, Gray PG, Lu GQ. Hydrothermally robust molecular sieving silica for wet gas separation. *Adv Funct Mater*. 2006;16:1215–1220.
17. Ockwig NW, Nenoff TM. Membranes for hydrogen separation. *Chem Rev*. 2007;107:4078–4110.
18. Tsuru T. Nano/subnano-tuning of porous ceramic membranes for molecular separation. *J Sol-Gel Sci Technol*. 2008;46:349–361.
19. Dong J, Lin YS, Kanezashi M, Tang Z. Microporous inorganic membranes for high temperature hydrogen purification. *J Appl Phys*. 2008;104:121301–121317.
20. Ohta Y, Akamatsu K, Sugawara T, Nakao A, Miyoshi A, Nakao S. Development of pore size-controlled silica membranes for gas separation by chemical vapor deposition. *J Membr Sci*. 2008;315:93–99.
21. Castricum HL, Sah A, Kreiter R, Blank DHA, Vente JF, ten Elshof JE. Hydrothermally stable molecular separation membranes from organically linked silica. *J Mater Chem*. 2008;18:2150–2158.
22. Kanezashi M, Yada K, Yoshioka T, Tsuru T. Design of silica networks for development of highly permeable hydrogen separation membranes with hydrothermal stability. *J Am Chem Soc*. 2009;131:414–415.
23. Asaeda M, Yamasaki S. Separation of inorganic/organic gas mixtures by porous silica membranes. *Sep Purif Technol*. 2001;25:151–159.
24. Kanezashi M, Asaeda M. Stability of H_2-permeselective Ni-doped silica membranes in steam at high temperature. *J Chem Eng Jpn*. 2005;38:908–912.
25. Kanezashi M, Asaeda M. Hydrogen permeation characteristics and stability of Ni-doped silica membranes in steam at high temperature. *J Membr Sci*. 2006;271:86–93.
26. Igi R, Yoshioka T, Ikuhara YH, Iwamoto Y, Tsuru T. Characterization of Co-doped silica for improved hydrothermal stability and application to hydrogen separation membranes at high temperatures. *J Am Ceram Soc*. 2008;91:2975–2981.
27. Yoshioka T, Tsuru T, Asaeda M. Molecular dynamics studies on gas permeation properties through microporous silica membranes. *Sep Purif Technol*. 2001;25:441–449.
28. Yoshioka T, Nakanishi E, Tsuru T, Asaeda M. Experimental study of gas permeation through microporous silica membranes. *AIChE J*. 2001;47:2052–2063.
29. Shelekhin AB, Dixon AG, Ma YH. Theory of gas diffusion and permeation in inorganic molecular-sieve membranes. *AIChE J*. 1995;41:58–67.
30. Hacarlioglu P, Lee D, Gibbs GV, Oyama ST. Activation energy for permeation of He and H_2 through silica membranes. *J Membr Sci*. 2008;313:277–283.
31. Brodka A, Zerda TW. Molecular dynamics of SF_6 in porous silica. *J Chem Phys*. 1991;95:3710–3718.

Manuscript received Jun. 16, 2009, and revision received July 26, 2009.